Pushing a Robot Along - A Natural Interface for Human-Robot Interaction

Julien Frémy
Dept. of Electrical & Computer Eng.
Université de Sherbrooke
Sherbrooke, QC - CANADA
Email: julien.fremy@usherbrooke.ca

François Michaud
Dept. of Electrical & Computer Eng.
Université de Sherbrooke
Sherbrooke, QC - CANADA
Email: francois.michaud@usherbrooke.ca

Michel Lauria
University of Applied Sciences
Western Switzerland (HES-SO)
Geneva Switzerland
Email: michel.lauria@hesge.ch

***Abstract*— Humans use direct physical interactions to move objects and guide people, and the same should be done with robots. However, most of today's mobile robots use non-backdrivable motors for locomotion, making them potentially dangerous in case of collision. This paper presents a robot, named AZIMUT-3, equipped with differential elastic actuators that are backdrivable and torque controlled, capable of being force-guided. Real world results demonstrate that AZIMUT-3 can move efficiently in response to physical commands given by a human pushing the robot in the intended direction.**

I. INTRODUCTION

To make robots move from industrial to natural settings, they must be able to interact safely and naturally in physical contact with people. Most mobile robots are still actuated with motors that are not backdrivable. Thus, when a contact occurs between the robot and an object or a human being, both the motors and the encountered entity must be able to sustain the shock. To do so, mobile platforms limit their velocities or rely on sensors to perceive the operating environment with sufficient precision to avoid potential accidents.

However, humans use direct physical interactions to influence their motion. For instance, guiding someone by holding his/her hand or shoulders is very common. Such natural interface would be beneficial for mobile robots too, instead of relying on remote controllers (e.g., joysticks, gamepads) or having to physically carry the robot. In such a scenario, the robot's motors should be put to use for moving in the direction given by someone physically guiding the robot. Such a platform must be able to safely support physical contacts, and respond appropriately. Such capabilities are inherently applicable to mobile devices such as motorized carts, electric wheelchairs, etc.

This paper presents a pseudo-omnidirectional mobile platform, named AZIMUT-3, that can detect forces on the horizontal plane to move in the intended direction. The platform uses steerable wheels motorized using differential elastic actuators (DEA) [1], which provide compliance, safety and torque control capabilities. This design provides a natural physical interface without requiring the use of costly sensors such as six Degrees Of Freedom (DOF) force/torque sensors.

The paper is organized as follows. Section II is an overview of existing force-guided systems, such as object-transportation and walking assistant devices. Section III introduces our platform and its characteristics. Section IV describes its control approach, allowing it to sense the forces through the DEAs and generating commands to assist or restrain motion of the platform. Section V presents real world evaluations of the system, demonstrating the feasibility of the approach.

II. FORCE-GUIDED MOBILE ROBOTS

Passive robots, i.e., robots that can steer their joints but require a human to propel it, are one category of machines that are physically force-guided. The Passive Robot PRP [2], is one example. This omnidirectional robot uses brakes on its wheels to steer them in the desired direction, sensed using a 6 DOF force/torque sensor. A similar system is used in RT-Walker [3], with force sensors installed in handle bars to detect user's intent. Guido [4], a walking assistant, embeds a force sensor in its handle bars to determine how to steer the robot, and uses speakers to interact vocally with the user. Finally, Wasson's COOL-Aide [5] uses two 6 DOF force and torque sensors to steer and brake the platform based on user's intent and the environment. One drawback of passive robots is that their propulsion is provided by their users, limiting their usage and the equipment they can carry.

Active robots, on the other hand, provide propulsion to the platform, making it possible to assist user's motion. MOBIL [6] is a differential drive robot that assists its user in walking and moving objects. It does so using two joysticks equipped with force sensors to assess user's intent. Smartwalker [7] is an omnidirectional device based on two caster wheels. It uses a 6 DOF force/torque sensor and speakers to interact with its user. Its suspension allows it to evolve safely on uneven floors. CMU Robotic Walker [8] is based on a Nomadic XR-4000, an omnidirectional platform based on four caster wheels, and uses a screen and a set of force sensors in its handle bars for interaction with the user. Walking Helper [9] is also omnidirectional and uses multi-axis force sensors in the handle bars. In all these robots, force and torque sensors are integrated in the handle bars, limiting the application of forces to a very specific location on the robot, and altering the simplicity of a direct physical interaction. Such a setup also requires some form of training and the use of sophisticated force/torque sensor and control systems.

III. AZIMUT-3

AZIMUT-3 is a pseudo-omnidirectional platform [10] that can be considered an alternative solution to active, force-guided robots. It is made of four steerable wheels called AZIMUT wheels [11]. They permit to lower the height of the chassis of AZIMUT-3. Compared to other wheels that can provide omnidirectionality, they are lighter and mechanically simpler than Swedish wheels and allow to have some kind of simple horizontal suspension system impossible to retrieve with active caster wheels.

Each AZIMUT wheel has two motors : a classical DC brushless motor to propel the wheel and a DEA to steer the wheel. A DEA is conceptually similar to Series Elastic Actuator (SEA) [12] [13], but uses a differential coupling instead of a serial coupling between a high impedance mechanical servomotor and a low impedance mechanical spring. This results in a more compact and simpler solution, with similar performances. DEA allows to control its mechanical elasticity and viscosity, in accordance with the admittance control scheme as expressed by (1),

$$\frac{X(s)}{F(s)} = \frac{1}{Ds + K} \tag{1}$$

where F is the force sensed (provided by a MLP-300 load cell from Transducer Techniques) on the output of the DEA, D and K are the chosen damping and viscosity, and X is the steer angle at the output of the DEA that describes the orientation of the wheel (provided by a RM44 wheel encoder from RLS). The DC motor used in DEAs is a K064-050 provided by Bayside. This makes DEA acts as an active elastic element that can inherently absorb shocks and perceive the forces coming from the environment.

Fig. 1 shows AZIMUT-3 equipped with a handle bar free of any sensors, except a 6 DOF force sensing device (Mini-45 SI-290-10 from ATI Automation) used for ground truth monitoring only. Each wheel is equipped with a propulsion motor (also a K064-050 from Bayside) and a wheel encoder (E4 from US Digital allowing a resolution of 60000 pulses per revolution), and is capable of reaching 1.47 m/s. AZIMUT-3's hardware architecture consists of distributed modules for sensing and low-level control, communicating with each other through a 1 Mbps CAN bus. A Mini-ITX computer equipped with a 2.0 GHz Core 2 duo processor running Real-time Linux is used on-board for high-level control modules running as threads and communicating through Qt's event system. Nickel-metal hybrid batteries provides power to the platform for 2 to 3 hours of autonomy. A passive vertical suspension mechanism (Rosta springs) is used to connect the wheels to AZIMUT's chassis, allowing them to keep contact with the ground on uneven surfaces. The platform has a 34 kg payload capacity.

As shown in Fig. 2, the DEAs steer the wheels of AZIMUT-3 and can perceive forces applied on them around their rotation axis. However, if a force is applied in the same direction than the wheel axis direction, there will be no resulting torque on the DEA steering axis, and the force cannot be detected. Fig. 2 also illustrates the range of motion of each steerable wheel on the plane of motion of AZIMUT-3. To allow such a robot to move, we must have a configuration in which all the wheels' axis must either converge in one point called Instantaneous Center of Rotation (ICR), or be all parallel (the ICR is then at an infinite distance of the robot). Because there are discontinuities in the wheels' orientations depending on where the ICR is on the plane of motion (see Fig. 3), we have divided this plane in three sections called modes [11]:

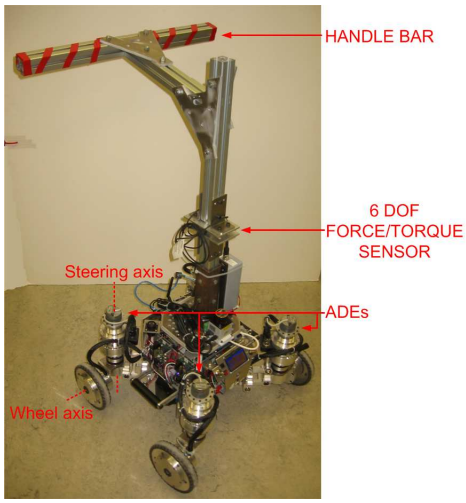

Fig. 1. AZIMUT 3 and its handle.

- With Mode 1, the ICR is defined on two triangular sections of the plane. This mode is used for moving forward on straight lines.
- Mode 2 is similar to Mode 1, but rotated 90 degrees around the center of the robot. This mode is used to move perpendicularly to its forward direction.
- Mode 3 allows the platform to make tight turning maneuvers and rotate on itself.

An ICR must be defined to allow AZIMUT-3 to move, thus we have decided that its commands will take the form of an ICR along with a velocity, which completely defines the desired move.

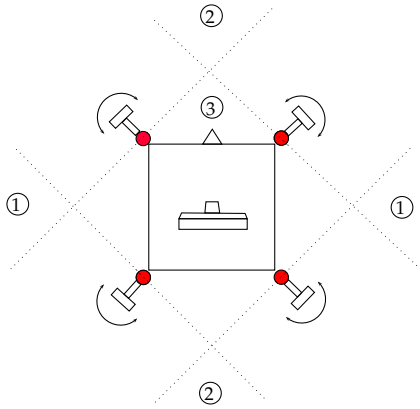

Fig. 2. Top view representation of AZIMUT-3, with its handle bar.

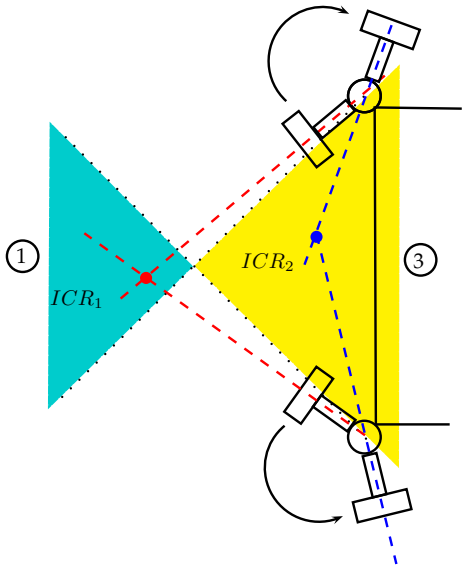

Fig. 3. ICR defined in Mode 1 and Mode 3. Close ICRs in the plane of motion can lead to discontinuities in the orientation of the wheels.

IV. FORCE-GUIDED CONTROL

To control AZIMUT-3 according to forces and torques applied on the platform, we have artificially constrained the ICR to belong to two half lines (see Fig. 4), restricting allowable motion to portions of Mode 1. We selected this mode because it is common for people to push an object from the back (e.g., shopping carts, wheelchairs). Moreover, because a transition between modes requires the platform to come to a stop, we limited our first study to only Mode 1 to ensure motion smoothness and simplicity. Finally, limits on force detection explained at the end of the mechanical analysis lead us to only detect forces along one dimension and thus reducing Mode 1 to two half-lines instead of the two original triangular surfaces.

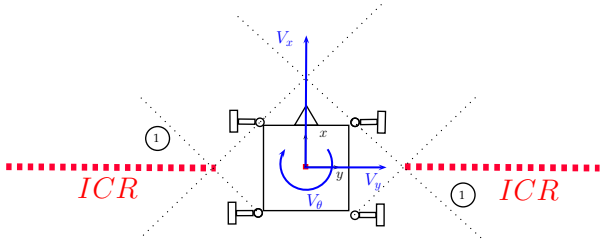

Fig. 4. Restricted ICR space.

The algorithm for force-guiding AZIMUT-3's consists of the following four steps.

1) Filtering of torque readings: Torque data sensed through AZIMUT-3's DEA are the inputs from which our algorithm has to determine user's intent. A dead zone and a fourth order Chebychev filter are used to remove noise and residual torques that can arise from frictions in the actuators. These manipulations permit to have $\boldsymbol{\tau}'$, the torques measured and pre-processed.

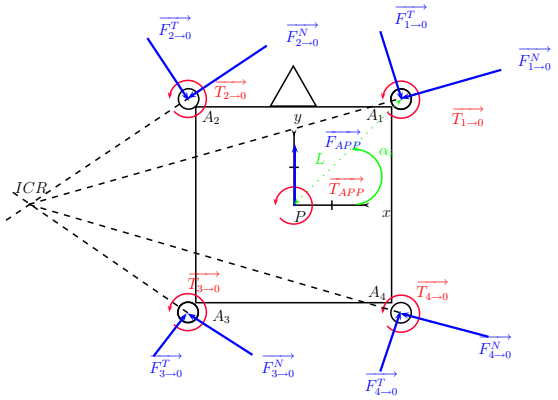

Fig. 5. Mechanical analysis of the chassis of AZIMUT-3.

2) Computation of force and torque exerted by the user: To retrieve from $\boldsymbol{\tau}'$ the forces exerted on the platform, we make a mechanical analysis of our robot with the two following assumptions :

1) The efforts of dynamics are not significant.
2) The component of reactions forces coming from the ground which is co-linear with the wheel axis is ignored.

The analysis has three main steps. First, it applies Newton's second law to a system composed only by the chassis of AZIMUT-3, as shown in Fig. 5. Thus, we have the sum of the forces and the sum of the torques applied to the chassis which are nil, as expressed by (2) and (3).

$$\overrightarrow{0} = \overrightarrow{F_{APP}} + \sum_{i=1}^{4} \overrightarrow{F_{i\to0}} \tag{2}$$

$$\overrightarrow{0} = \overrightarrow{T_{APP}} + \sum_{i=1}^{4} \overrightarrow{T_{i\to0}} + \sum_{i=1}^{4} \overrightarrow{PA_i} \times \overrightarrow{F_{i\to0}} \tag{3}$$

where :

$$\overrightarrow{F_{i\to0}} = \overrightarrow{F^T_{i\to0}} + \overrightarrow{F^N_{i\to0}} \tag{4}$$

Next, we apply Newton's second law to the wheel alone. The forces and moments considered are shown in Fig. 6, and their respective sums are nil, as expressed by (5) and (6) :

$$\overrightarrow{0} = \overrightarrow{F_{0\to i}} + \overrightarrow{F_{GND\to i}} \tag{5}$$

$$\overrightarrow{0} = \overrightarrow{T_{0\to i}} + \overrightarrow{G_iA_i} \times \overrightarrow{F_{0\to i}} + \overrightarrow{G_iB_i} \times \overrightarrow{F_{GND\to i}} \tag{6}$$

where :

$$\overrightarrow{F_{0\to i}} = \overrightarrow{F^T_{0\to i}} + \overrightarrow{F^N_{0\to i}} \tag{7}$$

$$\overrightarrow{F_{GND\to i}} = \overrightarrow{F^T_{GND\to i}} + \overrightarrow{F^N_{GND\to i}} \tag{8}$$

Finally, the third step combines the results of the first equalities with the assumptions made. After several manipulations, we obtain the equality on $\mathcal{F}_{G_i}$ $\overrightarrow{F_{0\to i}}$ given by (9), which is the expression of the vector $\overrightarrow{F_{0\to i}}$ in the frame $\mathcal{F}_{G_i}$

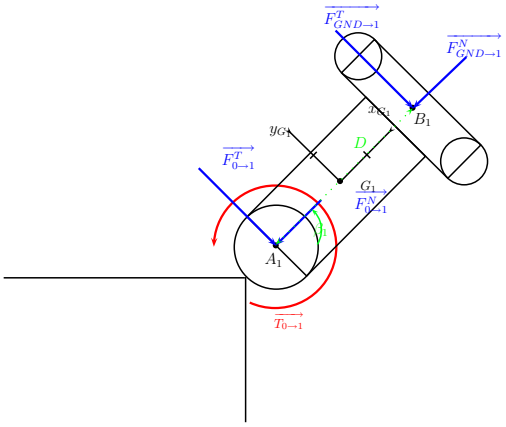

Fig. 6. Mechanical analysis of a single wheel of AZIMUT-3.

defined by G_i and the axes noted x_{G_i} and y_{G_i} shown in Fig. 6.

$$^{\mathcal{F}_{G_i}}\overrightarrow{F_{0\to i}} = \begin{pmatrix} 0 \\ -\frac{T_{0\to i_z}}{D} \\ 0 \end{pmatrix} \tag{9}$$

with :

$$\overrightarrow{T_{0\to i}} = \begin{pmatrix} 0 \\ 0 \\ T_{0\to i_z} \end{pmatrix} \tag{10}$$

(10) is valid in both frames ($\mathcal{F}_P$ defined by Fig. 5 and $\mathcal{F}_{G_i}$), because their z-axis are parallel.

There is a rotation of $-\beta_i$ between $\mathcal{F}_P$ and $\mathcal{F}_{G_i}$, allowing us to define $^{\mathcal{F}_P}\overrightarrow{F_{0\to i}}$. With Newton's third law, we can determine $^{\mathcal{F}_P}\overrightarrow{F_{i\to 0}}$ and $\overrightarrow{T_{i\to 0}}$:

$$\overrightarrow{F_{0\to i}} = -\overrightarrow{F_{i\to 0}} \tag{11}$$

$$\overrightarrow{T_{0\to i}} = -\overrightarrow{T_{i\to 0}} \tag{12}$$

Thus, we can express (2) and (3) with (13) :

$$\overrightarrow{F_{APP}} = \begin{pmatrix} F_{APP_x} \\ F_{APP_y} \\ 0 \end{pmatrix} = \begin{pmatrix} \sum_{i=1}^{4} -\frac{T_{0\to i_z}}{D}.sin(\beta_i) \\ \sum_{i=1}^{4} -\frac{T_{0\to i_z}}{D}.cos(\beta_i) \\ 0 \end{pmatrix} \tag{13}$$

$$\overrightarrow{T_{APP}} = \sum_{i=1}^{4} \overrightarrow{T_{0\to i}} - \sum_{i=1}^{4} \begin{pmatrix} 0 \\ 0 \\ -L.\frac{T_{0\to i_z}}{D}.cos(^{\mathcal{F}_P}\alpha_i + \beta_i) \end{pmatrix} \tag{14}$$

L, α_i (see Fig. 5) and D (see Fig. 6) are static parameters of the robot that are known. $T_{0\to i_z}$ tally with the available $\boldsymbol{\tau'}$ and β_i are also measured by the DEAs. Therefore, we have at our disposal the value of the force and the torque applied by the environment (e.g., a user pushing the robot in our case) on the platform.

As expressed by (13), the detection of the force is limited because of the wheels orientation represented by β_i. Indeed, trying to determine F_x when all the $sin(\beta_i)$ are nil is impossible.

3) Generating a command based on the applied forces: Based on the force and torque perceived, direction (for the steerable wheels) and propulsion commands must be generated to assist motion in the intended direction. We have decided to represent these commands as twists, a common notation for the velocity of a robot, as expressed in 15.

$$\overrightarrow{t} = \begin{pmatrix} V_x \\ V_y \\ V_\theta \end{pmatrix} \tag{15}$$

The frame in which we define velocities of the robot is rotated 90 degrees counterclockwise with the frame shown in Fig. 5. Our algorithm calculates a translational velocity V_y and a rotational speed V_θ, with V_x set to 0 (because our ICR space is limited to two half lines, there is no lateral velocity). The values of force and torque computed are provided to controllers similar to [7] and [9]. These controllers introduce a translational damping D_{LTF} and a mass M_{LTF} that make the robot behave like an object that would have those damping and mass, in a world where no other other forces would act (i.e., without gravity).. The transfer functions for V_y and V_θ are given by (16) and (17) :

$$\frac{V_y(s)}{F_{APP}(s)} = \frac{1}{M_{LTF}s + D_{LTF}} \tag{16}$$

$$\frac{V_\theta(s)}{T_{APP}(s)} = \frac{1}{J_{ATF}s + D_{ATF}} \tag{17}$$

with J_{ATF} and D_{ATF} representing the inertia and the angular damping desired.

4) Converting a twist into an ICR: As specified in Section III, AZIMUT-3 commands are ICRs defined in $\mathcal{F}_P$. It is simpler to measure an ICR using polar coordinates with ρ as the radial coordinate and γ as the angular coordinate.

To obtain ρ and γ from V_y and V_θ, our algorithm uses an approach similar to [14], converting twist components into a spherical ICR representation using a gnomonic projection, expressed by (18) and (19).

$$X_{ICR} = \frac{-V_y}{\sqrt{V_y^2 + V_\theta^2}} \tag{18}$$

$$Z_{ICR} = \frac{-V_\theta}{\sqrt{V_y^2 + V_\theta^2}} \tag{19}$$

Because we have reduced the possible positions of the ICR on two line portions (the ICR space of Fig. 4), the projection sphere is reduced to two arcs of a circle in a plane perpendicular to the plane of motion of AZIMUT-3 containing P, as shown by Fig. 7. We have also removed its lower hemisphere so as to always obtain only one possible solution. X_{ICR} and Z_{ICR} are the cartesian coordinates of the intersection between the line formed by the ICR and O (center of the reduced projection sphere) and the arcs of circle defined in the frame of center O.

ρ and γ are then directly given by :

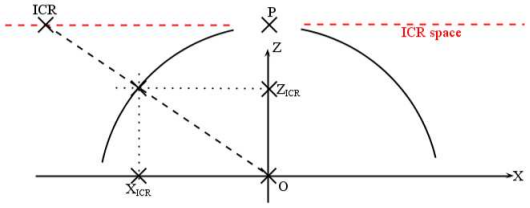

Fig. 7. Transposition from spherical coordinates to ICR.

$$\rho = \frac{X_{ICR}}{Z_{ICR}} \tag{20}$$

$$\gamma = \begin{cases} 0 & \text{if } X_{ICR} > 0; \\ \pi & \text{if } X_{ICR} < 0. \end{cases} \tag{21}$$

Along with the position of the ICR, we need the chassis velocity p_v, expressed as a percentage of the maximum velocity of the robot and is computed using (22):

$$p_v = \frac{m}{m_{max}} \tag{22}$$

where m is :

$$m = \pm\sqrt{V_y^2 + V_\theta^2} \tag{23}$$

and m_{max} is an ICR dependent value computed for each wheel and taking into account the physical limits of motors propelling the wheels to avoid saturation of one of them, while making sure they are used to their full velocity range.

V. RESULTS

A. Validation of the force and torque computation

Fig. 8 and Fig. 9 compare the forces exerted on the platform computed with our algorithm and the force measured with the 6 DOF force sensing device installed under the handle bar. These figures show that our algorithm gives a good approximation of the forces and torques exerted on the device. However, we observe a minor delay (around 0.1 s) between the measures, which is mainly due to elasticity of the DEA which absorb a portion of the forces applied.

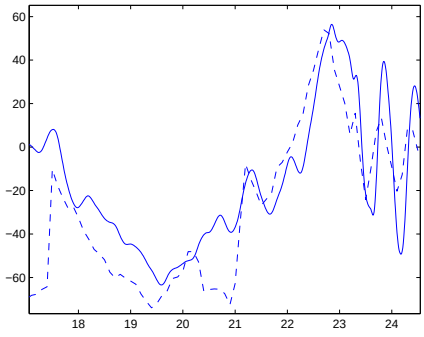

Fig. 8. Computed translational force (solid) and measured translational force in N (dash) versus time in s.

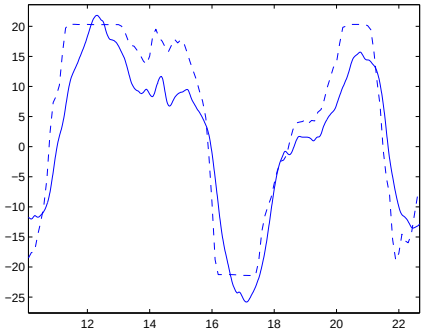

Fig. 9. Computed rotational torque (solid) and measured rotational torque in Nm (dash) versus time in s.

B. Validation of the Commands Generated based on the Applied Forces

The velocities generated by the applied forces can be seen in Fig. 10 and Fig. 11. The apparent mass and damping were set to 10 kg and 9 kg/s, the apparent inertia and angular damping were set to 5 kg.m^2 and 30 kg.m^2/s. These values allowed to have an increased stability but makes the device heavy. The maximum velocity was set at 0.5 m/s. As expected, the algorithm described by (16) and (17) behave like low-pass filters to smooth the velocity commands. Additionally, the device remains responsive because a change in the torque applied is followed within around 50 ms by a change in the velocity command.

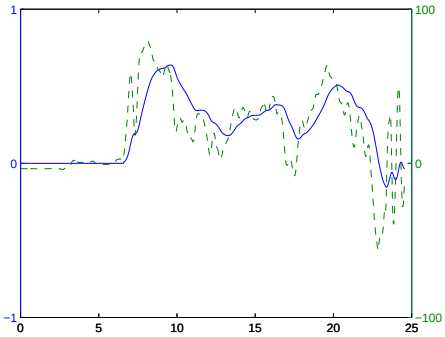

Fig. 10. Computed translational velocity in m/s (solid) and applied translational force in N (dash, labels on the right axis) versus time in s.

C. Trials with the Complete System

To validate the functionality of our algorithm, we asked 7 non-experimented users of the platform to force-guide the platform, following a path as accurately and as fast as possible, with an obstacle to be avoided and handle a tight turn. Translational and rotational velocities and trajectories for each trials were recorded. The parameters are the same as in the experiment presented in Section V-B. In all cases, the goal has been reached with an average speed of 0.15 m/s.

Fig. 13 shows an example of a trial. The red markers shows the connection between the velocity and the position, shown

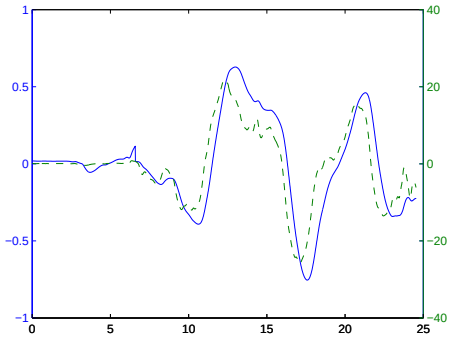

Fig. 11. Computed rotational velocity in m/s (solid) and applied rotational torque in Nm (dash, labels on the right axis) versus time in s.

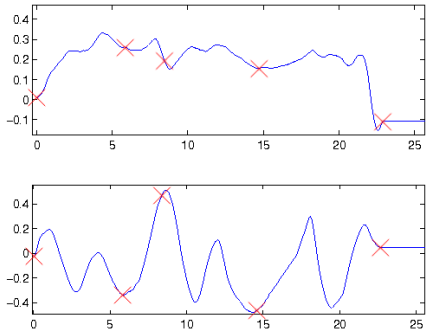

Fig. 13. Translational velocity in m/s (top) and rotational computed velocity in rad/s (bottom) versus time in s for a trial.

in Fig. 12. After the initial acceleration, the translational velocity remains relatively constant, a constant speed during the experiment, to then decelerate and stop. The rotational velocity shows the efforts made by the user to stay on the path. In Fig. 12, it can be observed that the second turn is more difficult to do. This can be explained by limitations of our algorithm on very precise motions. Firstly, the filtering done on the torque measures, while protecting from persistent torques in the DEA, rejects the low applied efforts on the device. Secondly, the constraint on V_θ implied by the obligation to stay in Mode 1 limits the mobility of the device for the low translational velocities that the users had for this sharp turn.

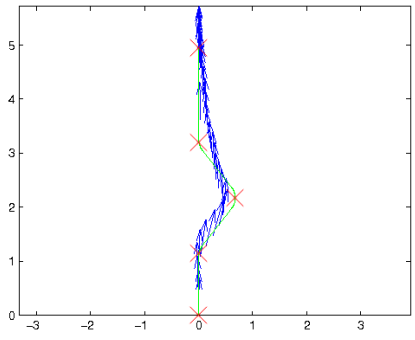

Fig. 12. Path to follow (green) and mean path of the 7 users with orientation (blue). Start is at (0, 0) end arrival is at (0, 5). Units are in m.

VI. CONCLUSION AND FUTURE WORK

Using AZIMUT-3 as an experimental platform, this paper demonstrates that it is possible to exploit the capabilities of differential elastic actuators for motorization of steerable wheels, to make a mobile platform respond to forces and torques from a human physically guiding the robot. Encouraged by these results, our next step is to integrate, in our control algorithm, transitions between modes to allow various moves. We also want to use the algorithm in a control architecture that would allow the platform to be physically guided while avoiding obstacles (detected using a laser range finder), and that can operate on incline surfaces (detected using an inclinometer).

ACKNOWLEDGMENTS

F. Michaud holds the Canada Research Chair on Mobile Robotics and Autonomous Intelligent Systems. This project is funded by the Natural Sciences and Engineering Research Council of Canada and the Canadian Foundation for Innovation.

REFERENCES

[1] M. Lauria, M. Legault, M. Lavoie, and F. Michaud, “Differential elastic actuator for robotic interaction tasks,” pp. 3606–3611, 2008.
[2] Z. Wang, K. Fukaya, Y. Hirata, and K. Kosuge, “Control passive mobile robots for object transportation - Braking torque analysis and motion control,” pp. 2874–2879, 2007.
[3] Y. Hirata, A. Hara, and K. Kosuge, “Motion control of passive intelligent walker using servo brakes,” *IEEE Trans. on Robotics*, vol. 23, no. 5, pp. 981–990, 2007.
[4] G. Lacey and D. Rodriguez-Losada, “The evolution of Guido,” *IEEE Robotics & Automation Magazine*, vol. 15, no. 4, pp. 75–83, 2008.
[5] G. Wasson, P. Sheth, M. Alwan, K. Granata, A. Ledoux, and C. Huang, “User intent in a shared control framework for pedestrian mobility aids,” pp. 2962–2967, 2003.
[6] A. Sabatini, V. Genovese, and E. Pacchierotti, “A mobility aid for the support to walking and object transportation of people with motor impairments,” pp. 1349–1354, 2002.
[7] M. Spenko, H. Yu, and S. Dubowsky, “Robotic personal aids for mobility and monitoring for the elderly,” *IEEE Trans. on Neural Systems and Rehabilitation Engineering*, vol. 14, no. 3, pp. 344–351, 2006.
[8] A. Morris, R. Donamukkala, A. Kapuria, A. Steinfeld, J. Matthews, J. Dunbar-Jacob, and S. Thrun, “A robotic walker that provides guidance,” pp. 25–30, 2003.
[9] O. Chuy, Y. Hirata, and K. Kosuge, “Active type robotic mobility aid control based on passive behavior,” pp. 165–170, 2007.
[10] Y. Mori, E. Nakano, and T. Takahashi, “Mechanism, control and design methodology of the nonholonomic quasi-omnidirectional vehicle ’ODV9’,” *The Int. Journal of Robotics Research*, vol. 21, no. 5-6, p. 511, 2002.
[11] M. Lauria, I. Nadeau, P. Lepage, Y. Morin, P. Giguere, F. Gagnon, D. Letourneau, and F. Michaud, “Kinematical analysis of a four steered wheeled mobile robot,” pp. 3090–3095, 2006.
[12] M. Williamson, “Series elastic actuators,” Ph.D. dissertation, Massachussetts Institute of Technology, Cambridge, Boston, 1995.
[13] D. Robinson, “Design and analysis of series elasticity in closed loop actuator force control,” Ph.D. dissertation, Massachussetts Institute of Technology, Cambridge, Boston, 2000.
[14] C. P. Connette, A. Pott, M. Hagele, and A. Verl, “Control of an pseudo-omnidirectional, non-holonomic, mobile robot based on an ICM representation in spherical coordinates,” pp. 4976–4983, 2008.